The Journal of Physiology

Individual variability of cerebral autoregulation, posterior cerebral circulation and white matter hyperintensity

Jie Liu[1,2,3], Benjamin Y. Tseng[1,2], Muhammad Ayaz Khan[1,2], Takashi Tarumi[1,2], Candace Hill[1], Niki Mirshams[1], Timea M. Hodics[4], Linda S. Hynan[5] and Rong Zhang[1,2,4]

[1]*Institute for Exercise and Environmental Medicine, Texas Health Presbyterian Hospital Dallas, Dallas, TX, USA*
[2]*Department of Internal Medicine, University of Texas Southwestern Medical Centre, Dallas, TX, USA*
[3]*Department of Ultrasound Diagnostics, Tangdu Hospital, Fourth Military Medical University, Xi'an, China*
[4]*Department of Neurology and Neurotherapeutics, University of Texas Sothwestern Medical Centre, Dallas, TX, USA*
[5]*Department of Clinical Sciences and Psychiatry, University of Texas Southwestern Medical Centre, Dallas, TX, USA*

Key points

- Cerebral autoregulation (CA) is a key mechanism to protect brain perfusion in the face of changes in arterial blood pressure, but little is known about individual variability of CA and its relationship to the presence of brain white matter hyperintensity (WMH) in older adults, a type of white matter lesion related to cerebral small vessel disease (SVD).
- This study demonstrated the presence of large individual variability of CA in healthy older adults during vasoactive drug-induced changes in arterial pressure assessed at the internal carotid and vertebral arteries. We also observed, unexpectedly, that it was the 'over-' rather than the 'less-reactive' CA measured at the vertebral artery that was associated with WMH severity.
- These findings challenge the traditional concept of CA and suggest that the presence of cerebral SVD, manifested as WMH, is associated with posterior brain hypoperfusion during acute increase in arterial pressure.

Abstract This study measured the individual variability of static cerebral autoregulation (CA) and determined its associations with brain white matter hyperintensity (WMH) in older adults. Twenty-seven healthy older adults (13 females, 66 ± 6 years) underwent assessment of CA during steady-state changes in mean arterial pressure (MAP) induced by intravenous infusion of sodium nitroprusside (SNP) and phenylephrine. Cerebral blood flow (CBF) was measured using colour-coded duplex ultrasonography at the internal carotid (ICA) and vertebral arteries (VA). CA was quantified by a linear regression slope (CA slope) between percentage changes in cerebrovascular resistance (CVR = MAP/CBF) and MAP relative to baseline values. Periventricular and deep WMH volumes were measured with T2-weighted magnetic resonance imaging. MAP was reduced by −11 ± 7% during SNP, and increased by 21 ± 8% during phenylephrine infusion. CA demonstrated large individual variability with the CA slopes ranging from 0.37 to 2.20 at the ICA and from 0.17 to 3.18 at the VA; no differences in CA were found between the ICA and VA. CA slopes measured at the VA had positive correlations with the total and periventricular WMH volume ($r = 0.55$ and 0.59, $P < 0.01$). Collectively, these findings demonstrated the presence of large individual variability of CA in older adults, and that, when measured in the posterior cerebral circulation, it is the higher rather than lower CA reactivity that is associated with WMH severity.

DOI: 10.1113/JP271068

(Received 10 June 2015; accepted after revision 5 January 2016; first published online 11 January 2016)
Corresponding author R. Zhang: Institute for Exercise and Environmental Medicine, Texas Health Presbyterian Hospital Dallas, 7232 Greenville Ave., Dallas, TX 75231, USA. Email: RongZhang@texashealth.org

Abbreviations Anti-HTN, anti-hypertensive medication; CA, cerebral autoregulation; CBF, cerebral blood flow; CBFV, cerebral blood flow velocity; CPP, cerebral perfusion pressure; CVR, cerebrovascular resistance; CVRI, cerebrovascular resistance index; $ETCO_2$, partial pressure of end-tidal carbon dioxide; DWMH, deep white matter hyperintensity; FLAIR, fluid-attenuated inversion recovery; ICA, internal carotid artery; ICP, intracranial pressure; ICV, intracranial volume; MAP, mean arterial pressure; MCA, middle cerebral artery; MRI, magnetic resonance imaging; PCA, posterior cerebral artery; PWMH, periventricular white matter hyperintensity; PWV, pulse wave velocity; SBP, systolic blood pressure; SNP, sodium nitroprusside; SVD, small vessel disease; TAMV, time-averaged mean velocity; TCD, transcranial Doppler; TWMH, total white matter hyperintensity; VA, vertebral artery; VRFs, vascular risk factors; WMH, white matter hyperintensity.

Introduction

Cerebral autoregulation (CA) refers to the intrinsic ability of cerebral vasculature to regulate its resistance to protect brain perfusion during changes in cerebral perfusion pressure (CPP), which equals the difference between mean arterial pressure (MAP) and intracranial pressure (ICP) (Paulson *et al.* 1990). Under normal conditions, ICP is small ($\sim$ 5–15 mmHg for an adult in the supine position) and relatively constant; thus, changes in MAP probably reflect changes in CPP, which have been used for assessing CA (Tzeng & Ainslie, 2014). Furthermore, assessment of CA during dynamic changes in arterial pressure has been referred to as dynamic CA, while that during steady-state changes in arterial pressure has been referred to as static CA (Tan & Taylor, 2014).

Traditionally, static CA has been represented by a sigmoid curve with a wide plateau between about 60 and 150 mmHg MAP in healthy individuals, indicating that cerebral blood flow (CBF) is maintained constant despite large changes in arterial pressure (Lassen, 1959). The presence of this 'autoregulatory plateau' has been considered to represent normal function of CA, while a shortened or loss of this plateau suggests impaired CA (we will use CA to represent static CA below unless specified otherwise) (Lam *et al.* 1997).

However, this widely accepted dogma has been challenged by several recent studies, which showed that CBF could not be maintained constant during even moderate changes in arterial pressure and that individual variability of CA existed in healthy individuals (Lucas *et al.* 2010; Liu *et al.* 2013). Previous studies in animals also observed individual variability of CA during reductions in arterial pressure (Jones *et al.* 2002).

Given the pivotal role of CA in CBF regulation, quantitative assessment of CA individual variability may reveal its clinical significance. In this respect, impairment of CA and brain hypoperfusion in older adults have been linked to cognitive decline and dementia (Girouard & Iadecola, 2006).

The high prevalence of brain white matter hyperintensity (WMH) in older adults, as manifested on T2-weighted magnetic resonance imaging (MRI), has been well recognized and is an established risk factor of age-related cognitive decline and dementia (Wen & Sachdev, 2004). However, the pathology of WMH is not completely understood, and has been attributed to cerebral small vessel disease (SVD) (Wardlaw *et al.* 2013). At present, the relationship between CA and WMH is not known, although a few studies suggested that impairment of CA may contribute to the development of WMH due to hypoperfusion or ischaemic insults (Pantoni & Garcia, 1997). Conversely, because SVD involves cerebral arteriolosclerosis (Thompson & Hakim, 2009), endothelial dysfunction (Hoth *et al.* 2007) and/or arterial stiffness (Rosano *et al.* 2013), which all are important mediators of CA, WMH can potentially be a marker of impaired CA.

In addition, CA may have regional differences despite the presence of the circle of Willis as well as other downstream collateral circulations (Baumbach & Heistad, 1985). However, previous studies of dynamic or static CA focused mainly on the global or regional CBF changes in the anterior cerebral circulation, i.e. measurement of CBF responses to changes in arterial pressure at the internal carotid (ICA) or the middle cerebral arteries (MCA) (Aries *et al.* 2010), and few studies have assessed CA in the posterior circulation (i.e. the vertebrobasilar system) (Haubrich *et al.* 2004; Sorond *et al.* 2005; Reinhard *et al.* 2008; Nakagawa *et al.* 2009; Lewis *et al.* 2015).

In the present study, we tested the hypothesis that there is an association between individual variability of CA and WMH in older adults. In addition, we determined whether associations between CA and WMH have regional differences. Regional CA was assessed by measuring CBF velocity (CBFV) using transcranial Doppler (TCD) at the MCA, and CBF using colour-coded duplex ultrasonography at the ICA and the vertebral artery (VA) during vasoactive drug-induced stepwise decreases or increases in arterial pressure.

Methods

Participants

Twenty-seven healthy older adults were recruited from the local community to participate after a comprehensive physical examination including 12-lead ECG and echocardiogram. Exclusion criteria included smoking, substance misuse, major neurological and psychiatric diseases (e.g. clinical diagnosis of stroke, severe depression, traumatic brain injury and dementia), carotid or vertebral arterial stenosis (> 50%, assessed with ultrasonography), major medical disorders, unstable heart diseases, uncontrolled hypertension (systolic blood pressure ≥ 160 mmHg or diastolic blood pressure ≥ 100 mmHg) (Chobanian *et al.* 2003), obstructive sleep apnoea and diabetes mellitus. A composite score of vascular risk factors (VRFs) was used to code each individual subject with 0 for no risk factors, 1 for treated hypertension or hypercholesterolaemia, and 2 for the presence of both factors. The factor of anti-hypertensive medications (anti-HTN) is coded as 0 for no use and 1 for use. This study conformed to the standards of the *Declaration of Helsinki* for medical research involving human subjects. All subjects signed the informed consent with the study protocol approved by the Institutional Review Boards of the UT Southwestern Medical Centre and Texas Health Presbyterian Hospital of Dallas. Subjects were asked to refrain from high-intensity exercise, alcohol and caffeinated drinks at least 24 h before any of the following examinations, which were performed within 3 months.

MRI measurements

Magnetization-prepared rapid acquisition gradient echo (MPRAGE) and fluid-attenuated-inversion-recovery (FLAIR) images were obtained on a 3T MR system (Philips Medical System, Best, The Netherlands), using a body coil for radiofrequency transmission and a eight-channel head coil with parallel imaging capability for signal reception.

MPRAGE images were taken using the following parameters: TR = 8.1 ms, TE = 3.7 ms, FA = 12°, FOV = 256 × 256 mm, number of slices = 160 (no gap), resolution = 1× 1 × 1 mm^3, SENSE factor = 2, and scan duration = 4 min. MPRAGE images were processed using FreeSurfer software. Details of the procedures for measuring brain tissue volume were as published previously (Desikan *et al.* 2006). Total brain-tissue volume was obtained as a sum of cortical and subcortical grey matter and white matter volumes including the brainstem and cerebellum.

The methods used to measure WMH have been described in detail previously (Tseng *et al.* 2013). Briefly, FLAIR images were acquired (TR/TI/TE = 11,000/2800/125 ms) in the axial plane with 24 slices with 5 mm slice thickness and interslice gap of 1 mm. The field of view was 230 × 230 mm, and matrix size was 512 × 512. WMH voxels were identified using a semi-automatic method to measure the periventricular WMH (PWMH) and deep WMH (DWMH) volumes based on the lesion locations and cluster continuation, and total WMH (TWMH) was calculated as PWMH + DWMH volume (DeCarli *et al.* 2005). The infratentorial regions (including the cerebellum and brainstem) were excluded because of the lack of WMH in these regions in our subjects, and the limitations of using FLAIR images for delineating WMH in these regions (Wen & Sachdev, 2004). Intracranial volume (ICV) was measured using the atlas-based spatial normalization procedures to delineate cerebral spinal fluid/skull borders, and used to normalize WMH volumes (Wardlaw *et al.* 2013).

Assessment of cerebral autoregulation

To assess CA, intravenous infusions of sodium nitroprusside (SNP) and phenylephrine were used to induce stepwise changes in arterial pressure (Liu *et al.* 2013). Briefly, after baseline data collection, SNP was started with an infusion rate of 0.25 μg kg^{-1} min^{-1} and then increased incrementally by 0.25 μg kg^{-1} min^{-1} until mean arterial pressure (MAP) was reduced by 25% from the baseline or by 20 mmHg whichever came first. After SNP infusion, a time interval of ≥ 20 min was provided to allow changes in haemodynamics returning to baseline. Then, phenylephrine infusion was started with 0.5 μg kg^{-1} min^{-1} and then increased incrementally by 0.5 μg kg^{-1} min^{-1} until MAP was increased by 30% from the baseline or by 25 mmHg, whichever came first.

Brachial arterial pressure was measured using sphygmomanometry (Tango+, SunTech, Morrisville, NC, USA) to monitor steady-state changes in arterial pressure which was used to assess CA. Beat-to-beat changes in arterial pressure were measured continuously from the middle finger using photoplethysmography (Finapres, Ohmeda, USA) to monitor dynamic changes in arterial pressure and to assist the assessment of safety of subjects during vasoactive drug infusion. TCD (DWL Elektronische Systeme, Singen, Germany) was used to measure CBFV (i.e. time-averaged peak blood flow velocity) in the MCA. A custom-made probe holder or a headgear (Spencer Technologies, Northborough, MA, USA) was used to prevent movements of TCD probe during the study. Analog signals of finger arterial pressure, CBFV, ECG (GE Solar 8000 M, Milwaukee, WI, USA), arterial blood oxygen saturation (S_{aO_2}) (Biox 3700, Ohmeda) and partial pressure of end-tidal carbon dioxide ($ETCO_2$) (Capnogard, Novametrix, Wallingford, CT, USA) were recorded continuously using a data acquisition system (Acknowledge, BIOPAC Systems, Goleta, CA, USA). Heart rate, brachial arterial pressure, S_{aO_2}, $ETCO_2$ and CBFV at the MCA were averaged throughout the

period of duplex ultrasonography data collection (~ 5–7 min) at the baseline and during each stage of steady-state changes in arterial pressure for data presentation and CA analysis.

During each stage of drug infusion, when blood pressure was stabilized, CBF was measured at the ipsilateral ICA and VA. A duplex ultrasonography system (CX-50, Philips Healthcare) with a 3 to 12 MHz linear array transducer was used to measure CBF at the ICA and VA (Liu *et al.* 2014). Briefly, CBFV, time-averaged mean blood flow velocity (TAMV) and mean luminal diameters of the ICA and VA from 3 to 5 consecutive cardiac cycles were measured at the locations close to the head, and volumetric CBF was calculated as $CBF = TAMV \times [(Diameter/2)^2 \times \pi] \times 60$. CA was quantified from the linear regression slope of percentage changes relative to baseline (Δ%) in CBF, CBFV, cerebrovascular resistance (CVR = MAP/CBF) or cerebrovascular resistance index (CVRI = MAP/CBFV) in response to either absolute or percentage changes in MAP (Lucas *et al.* 2010; Liu *et al.* 2013). Further data analysis focused on the assessment of CA based on the slope of ΔCVR%–ΔMAP% (referred to as 'CA slope' unless specified otherwise) to facilitate the classification and comparison of individual CA variability. Global CA was assessed by measuring ΔCBF% obtained from the sum of CBF at the ICA and VA in response to changes in MAP, assuming that CBF differences between the left and right sides of ICA and VA were small and did not change during changes in drug-induced changes in arterial pressure. Cardiac output was measured using an inert gas rebreathing technique (Innocor, Innovision A/S, Odense, Denmark) at the baseline and the end of each drug infusion in a subgroup of 15 subjects to assess its potential effects on changes in CBF (Ogoh *et al.* 2005).

Aortic arterial stiffness

Recent studies suggest that increase in aortic/central artery stiffness, independent of age, is an important risk factor of WMH which should be considered to assess the relationship between CA and WMH (King *et al.* 2013). Pulse wave velocity (PWV) was measured from the carotid–femoral segment (aortic PWV) to assess central artery stiffness using applanation tonometry (SphygmoCor V8.0; AtCor Medical, West Ryde, NSW, Australia). The validation of this method has been published previously (Wilkinson *et al.* 1998).

Data analysis

Pearson's product moment correlation coefficients (r, for continuous variables) or Spearman's rank correlation coefficients (ρ, for categorical or ordinal variables) were calculated to examine the bivariate correlations among the regional and global CA metrics, WMH, age, sex, VRFs, Anti-HTN, SBP and PWV. Multiple variable linear regression analysis was used to examine the relationship between CA metrics and WMH by controlling other covariates as identified from the bivariate correlation analyses ($P < 0.15$) or based on previous publications (Sorond *et al.* 2005; Purkayastha *et al.* 2013). The Kolmogorov–Smirnov test was used to examine the normality of individual CA distribution. One-way repeated ANOVA was used to compare the haemodynamic measurements among different stages of drug infusion and the CA metrics measured at the different arteries. One-way ANOVA also was used to compare the CA metrics, $ETCO_2$ and diameter changes among the tertiles of PWMH volumes (< 0.15 %ICV, low; 0.15–0.30 %ICV, moderate; and > 0.30 %ICV, high). The equality of the variance was assessed by Pitman's test (Bartko, 1994), and Bonferroni correction or Games–Howell tests were used for *post hoc* pairwise comparisons. Values are expressed as mean ± SD. Statistical significance was assumed when $P < 0.05$. Data were analysed using SPSS 21 (IBM SPSS Inc., Chicago, IL, USA).

Results

The demographic characteristics of study participants and MRI measurements of brain volume and WMH are presented in Table 1. Drug infusion-induced changes in MAP, relative to baseline, ranged from –11 ± 7 to 21 ± 8%. Changes in systemic and cerebral haemodynamics during SNP infusion are presented in Table 2, and during phenylephrine in Table 3. Cardiac output did not change throughout the experiment (4.62 ± 0.85 l min^{-1} at baseline; 4.61 ± 0.87 l min^{-1} at the end of SNP infusion; 4.64 ± 0.82 l min^{-1} at the end of phenylephrine infusion). Subjects had no adverse events or reported discomfort during the experiment.

Assessments of CA using different metrics at the MCA, ICA and VA are presented in Table 4. No differences were found among different arteries and between regional and global measurements for the same CA metrics. However, CA slopes assessed with CBFV at the ICA and VA were higher by ~ 20–30% than those with CBF, while CVRI slopes were lower by ~ 20–30% than those of CVR, suggesting that changes in ICA and VA resistance (diameters) during changes in arterial pressure play a role in CA and that CA would be underestimated if using either the CBFV or the CVRI indices from the MCA, ICA or VA (Table 4). These observations are consistent regardless of whether absolute or relative changes in MAP were used for CA assessment.

Large individual variability of CA was observed at both the ICA and the VA (Figs 1 and 2). The CA patterns could be classified into tertiles as: (1) an apparently normal CA (CA slope 0.5–1.5), (2) a less effective or inferior CA (CA slope < 0.5) and (3) an over-reactive

Table 1. Demographic characteristics and MRI measurements

Variable	Value ($n = 27$)
Demographics	
Age (years)	66 (6)
Female	13 (48%)
Height (cm)	171 (8)
Weight (kg)	78 (15)
Body mass index (kg m^{-2})	26.6 (4.1)
Mini-Mental State Exam Score	29.1 (0.8)
Aortic PWV (m s^{-1})	9.56 (2.07)
Medical history	
Treated hypercholesterolaemia	11 (41%)
Treated hypertension	11 (41%)
Anti-hypertensive medications	
ACE inhibitors	7 (26%)
Diuretics	5 (19%)
Calcium channel blockers	4 (15%)
β-Blocker	1 (4%)
Renin inhibitor	1 (4%)
Neuroimaging	
ICV (ml)	1583 (160)
TBV (ml)	1148 (111)
Total WMH (%ICV)	0.283 (0.203)
PWMH (%ICV)	0.253 (0.189)
DWMH (%ICV)	0.030 (0.044)
Baseline haemodynamics	
SBP (mmHg)	123 (16)
DBP (mmHg)	76 (10)
MAP (mmHg)	91 (11)
Heart rate (b.p.m.)	61 (9)
S_{aO_2} (%)	97 (2)
$ETCO_2$ (mmHg)	37 (4)
ICA	
Diameter (mm)	4.51 (0.66)
CBF (ml min^{-1})	226 (57)
CVR (mmHg min ml^{-1})	0.43 (0.14)
VA	
Diameter (mm)	3.10 (0.54)
CBF (ml min^{-1})	73 (31)
CVR (mmHg min ml^{-1})	1.59 (0.95)

Values are expressed as mean (SD) or number (percentage). Aortic PWV, carotid–femoral pulse wave velocity; ACE, angiotensin converting enzyme; ICV, intracranial volume; TBV, total brain-tissue volume; WMH, white matter hyperintensity; PWMH, periventricular WMH; DWMH, deep WMH; SBP, systolic blood pressure; DBP, diastolic blood pressure; MAP, mean arterial pressure; S_{aO_2}, arterial blood oxygen saturation; $ETCO_2$, partial pressure of end-tidal carbon dioxide; ICA, internal carotid artery; CBF, cerebral blood flow; CVR, cerebrovascular resistance (= MAP/CBF); VA, vertebral artery.

CA (CA slope > 1.5) (Figs 1 and 2). The distributions of individual CA slope satisfied the Kolmogorov–Smirnov normality tests at both the ICA and the VA ($P = 0.81$ and 0.53 for two-tailed asymptotic significance, respectively) with no significant differences in their mean values (1.08 ± 0.53 *vs.* 1.13 ± 0.84, $P = 0.75$), but the variance of CA in the VA was larger than that of ICA ($P = 0.02$) (Fig. 2*A*).

The bivariate correlation matrix revealed that CA slope at the VA was positively associated with age and aortic stiffness (Table 5). In addition, both posterior and global CA slopes were associated positively with PWMH and TWMH ($P < 0.05$), although this was not the case for anterior CA measured at the MCA or ICA (Table 5). Aortic stiffness, and CA metrics at the VA, PWMH and TWMH all were associated positively with age ($P < 0.05$). Females had lower SBP and higher PWMH and TWMH than males ($P < 0.05$). Both SBP and WMH were associated positively with aortic stiffness ($P < 0.05$).

Multiple variable linear regression analysis showed that after statistical adjustments for age, sex, SBP and aortic PWV, higher posterior and global CA slopes assessed with ΔCBF% were associated with lower PWMH (partial correlation coefficients: $r = -0.55$, $P < 0.01$ for VA; $r = -0.54$, $P < 0.05$ for global CA) and lower TWMH (partial correlation coefficients: $r = -0.52$ for VA; $r = -0.53$ for global CA, $P < 0.05$); conversely, higher CA slopes assessed with ΔCVR% were associated with higher PWMH (partial correlation coefficients: $r = 0.59$, $P < 0.01$ for VA; $r = 0.52$, $P < 0.05$ for global CA) and higher TWMH (partial correlation coefficients: $r = 0.55$ for VA; $r = 0.51$ for global CA, $P < 0.05$). Of note, anterior CA metrics (at the MCA or ICA) showed no associations with WMH. A representative FLAIR image of WMH and assessment of CA at the VA during increase in arterial pressure is shown in Fig. 3.

The tertile analysis showed that in individuals who had high PWMH, CA slopes measured at the VA were greater than those measured at the ICA (1.99 ± 0.93 *vs.* 1.14 ± 0.40, $P < 0.05$) (Fig. 2*B*); moreover, CA slopes measured at the VA were greater in the high than low or moderate PWMH groups (1.99 ± 0.93 *vs.* 0.76 ± 0.55, $P < 0.05$; and 1.99 ± 0.93 *vs.* 0.78 ± 0.42, $P < 0.05$). No differences in CA slopes at the ICA were observed among the three PWMH groups (Fig. 2*B*). Of note, CA slopes of ΔCBF% at the VA were negative in those who had high PWMH, and were significantly different from those who had low or moderate PWMH (Table 6). Finally, linear regression slopes of changes in $ETCO_2$, and ICA and VA diameters in response to changes in arterial pressure were similar among the three groups of PWMH (Table 6).

Discussion

This study assessed regional CAs in the anterior and posterior cerebral circulation and their associations with WMH in older adults. We observed large individual variability of CA in both the anterior and the posterior circulation. Besides the apparently normal and less effective (or inferior) CA patterns, we observed an unexpected pattern of 'over-reactive CA' in about

Table 2. Systemic and cerebral haemodynamics during sodium nitroprusside infusion

Variables \ Drug infusion		Baseline	Sodium nitroprusside (μg kg^{-1} min^{-1}) 0.25	0.50	0.75	1.00
Subjects	(*n*)	27	23	22	11	8
Systemic haemodynamics						
SBP	mmHg	123 ± 16	121 ± 15	117 ± 11*	115 ± 11	109 ± 13
	Δ%	0	−2 ± 6	−8 ± 9*	−7 ± 10	−7 ± 12
DBP	mmHg	76 ± 10	75 ± 8	70 ± 9*	66 ± 9	63 ± 9
	Δ%	0	−1 ± 7	−8 ± 8*	−12 ± 6	−11 ± 9
MAP	mmHg	91 ± 11	90 ± 9	85 ± 8*	82 ± 8	79 ± 10
	Δ%	0	−2 ± 5	−9 ± 7*	−10 ± 7	−9 ± 9
HR	b.p.m.	61 ± 9	64 ± 10*	69 ± 11*	72 ± 15	71 ± 13
	Δ%	0	6 ± 6*	13 ± 15*	12 ± 10	16 ± 6
S_{aO_2}	% (absolute)	97 ± 2	97 ± 2	96 ± 3	95 ± 3	96 ± 2
	Δ% (relative)	0	0.0 ± 1.6	−0.8 ± 2.1	−1.7 ± 2.0	−0.2 ± 2.1
$ETCO_2$	mmHg	37 ± 4	36 ± 4	35 ± 4*	35 ± 6	38 ± 3
	Δ%	0	−2 ± 5	−5 ± 6*	−8 ± 7	−7 ± 3
MCA						
CBFV	cm s^{-1}	53.2 ± 16.4	48.2 ± 11.4	48.0 ± 15.6*	49.5 ± 20.5	48.8 ± 13.9
	Δ%	0	−5 ± 7	−10 ± 9*	−17 ± 10	−16 ± 12
CVRI	mmHg s cm^{-1}	1.84 ± 0.50	1.98 ± 0.55	1.92 ± 0.52	1.84 ± 0.52	1.72 ± 0.35
	Δ%	0	4 ± 10	3 ± 12	9 ± 20	10 ± 17
ICA						
CBFV	cm s^{-1}	42.1 ± 9.5	41.4 ± 10.9	37.8 ± 10.0*	37.4 ± 9.3	35.0 ± 6.5
	Δ%	0	−3 ± 11	−10 ± 10*	−13 ± 10	−15 ± 10
CVRI	mmHg s cm^{-1}	2.30 ± 0.72	2.35 ± 0.80	2.40 ± 0.67	2.33 ± 0.67	2.30 ± 0.49
	Δ%	0	2 ± 11	3 ± 13	6 ± 17	7 ± 14
Diameter	mm	4.51 ± 0.66	4.50 ± 0.62	4.65 ± 0.68*	4.36 ± 0.60	4.68 ± 1.00
	Δ%	0	1.1 ± 3.2	2.6 ± 3.2*	5.6 ± 3.4	2.0 ± 2.6
CBF	ml min^{-1}	226 ± 57	226 ± 64	220 ± 60	196 ± 62	204 ± 70
	Δ%	0	1 ± 20	−5 ± 11	−2 ± 11	−12 ± 8
CVR	mmHg min ml^{-1}	0.43 ± 0.14	0.44 ± 0.17	0.42 ± 0.13	0.46 ± 0.16	0.43 ± 0.17
	Δ%	0	0 ± 15	−3 ± 12	−7 ± 14	3 ± 13
VA						
CBFV	cm s^{-1}	26.5 ± 8.0	22.2 ± 6.5*	22.9 ± 5.2*	22.2 ± 6.5	22.1 ± 3.6
	Δ%	0	−12 ± 16*	−12 ± 16*	−19 ± 13	−17 ± 14
CVRI	mmHg s cm^{-1}	3.81 ± 1.49	4.50 ± 1.80*	3.93 ± 1.13	4.14 ± 1.84	3.61 ± 0.65
	Δ%	0	15 ± 24*	7 ± 22	14 ± 26	12 ± 20
Diameter	mm	3.10 ± 0.54	3.11 ± 0.57	3.12 ± 0.55	2.94 ± 0.48	3.18 ± 0.50
	Δ%	0	0.3 ± 3.0	0.9 ± 3.3	0.9 ± 3.8	−0.6 ± 2.6
CBF	ml min^{-1}	73 ± 31	64 ± 34	65 ± 27*	54 ± 21	65 ± 24
	Δ%	0	−9 ± 19	−9 ± 18	−17 ± 16	−18 ± 13
CVR	mmHg min ml^{-1}	1.59 ± 0.95	1.84 ± 1.07	1.59 ± 0.80	1.90 ± 1.18	1.38 ± 0.56
	Δ%	0	13 ± 29	5 ± 23	14 ± 32	13 ± 16
Global (ICA+VA)						
CBF	ml min^{-1}	299 ± 73	290 ± 80	285 ± 71	250 ± 65	268 ± 81
	Δ%	0	−1 ± 19	−6 ± 11	−6 ± 13	−14 ± 9
CVR	mmHg min ml^{-1}	0.33 ± 0.11	0.34 ± 0.14	0.32 ± 0.10	0.35 ± 0.13	0.31 ± 0.09
	Δ%	0	2 ± 17	−1 ± 13	−2 ± 17	6 ± 12

Values are mean ± SD, *$P < 0.05$, comparisons with the baseline using one-way repeated-measures ANOVA with Bonferroni correction for *post hoc* tests. Note that statistical analyses were performed only at the dosages of 0.25 and 0.50 μg kg^{-1} min^{-1} because fewer subjects had high dosages. The numbers of subjects were different at each stage because different dosages were required for them to reach the prior determined targets of changes in arterial pressure (see text). SBP, systolic blood pressure; Δ%, percentage change relative to baseline; DBP, diastolic blood pressure; MAP, mean arterial pressure; HR, heart rate; S_{aO_2}, arterial blood oxygen saturation; $ETCO_2$, partial pressure of end-tidal carbon dioxide; MCA, middle cerebral artery; ICA, internal carotid artery; VA, vertebral artery; CBFV, cerebral blood flow velocity; CVRI, cerebrovascular resistance index (= MAP/CBFV); CBF, cerebral blood flow; CVR, cerebrovascular resistance (= MAP/CBF).

Table 3. Systemic and cerebral haemodynamics during phenylephrine infusion

Variables \ Drug infusion		Baseline	Phenylephrine (μg kg^{-1} min^{-1}) 0.50	1.00	1.50
Subjects	(*n*)	27	25	21	6
Systemic haemodynamics					
SBP	mmHg	123 ± 16	137 ± 21†	150 ± 22†	156 ± 32
	Δ%	0	13 ± 9†	26 ± 13†	24 ± 7
DBP	mmHg	76 ± 10	81 ± 10†	86 ± 12†	83 ± 12
	Δ%	0	9 ± 9†	15 ± 10†	11 ± 9
MAP	mmHg	91 ± 11	100 ± 13†	107 ± 14†	107 ± 18
	Δ%	0	11 ± 9†	20 ± 10†	17 ± 7
HR	bpm	61 ± 9	57 ± 9†	57 ± 8	54 ± 4
	Δ%	0	−7 ± 10†	−6 ± 12	−5 ± 14
S_{aO_2}	% (absolute)	97 ± 2	98 ± 2†	98 ± 2†	98 ± 1
	Δ% (relative)	0	1.3 ± 1.8†	1.4 ± 2.0†	1.0 ± 1.2
$ETCO_2$	mmHg	37 ± 4	38 ± 3	38 ± 3	36 ± 5
	Δ%	0	0 ± 7	−1 ± 8	−3 ± 3
MCA					
CBFV	cm s^{-1}	53.2 ± 16.4	53.1 ± 14.9	52.4 ± 16.7	57.7 ± 24.3
	Δ%	0	−2 ± 11	−4 ± 10	−8 ± 9
CVRI	mmHg s cm^{-1}	1.84 ± 0.50	1.97 ± 0.46†	2.17 ± 0.55†	2.08 ± 0.69
	Δ%	0	13 ± 15†	25 ± 19†	28 ± 7
ICA					
CBFV	cm s^{-1}	42.1 ± 9.5	41.1 ± 9.4	39.7 ± 8.4	40.8 ± 5.9
	Δ%	0	−3 ± 12	−3 ± 11	−5 ± 7
CVRI	mmHg s cm^{-1}	2.30 ± 0.72	2.52 ± 0.56†	2.80 ± 0.65†	2.66 ± 0.51
	Δ%	0	16 ± 16†	25 ± 17†	24 ± 8
Diameter	mm	4.51 ± 0.66	4.49 ± 0.71	4.55 ± 0.76	4.85 ± 0.50
	Δ%	0	−0.7 ± 3.9	−0.7 ± 5.2	−1.8 ± 0.9
CBF	ml min^{-1}	226 ± 57	220 ± 62	220 ± 63	251 ± 50
	Δ%	0	−4 ± 13	−3 ± 14	−9 ± 10
CVR	mmHg min ml^{-1}	0.43 ± 0.14	0.48 ± 0.14†	0.53 ± 0.17†	0.44 ± 0.09
	Δ%	0	17 ± 18†	26 ± 25†	29 ± 10
VA					
CBFV	cm s^{-1}	26.5 ± 8.0	25.2 ± 7.0	26.9 ± 6.8	27.2 ± 6.5
	Δ%	0	−5 ± 19	4 ± 22	−1 ± 21
CVRI	mmHg s cm^{-1}	3.81 ± 1.49	4.31 ± 1.51†	4.28 ± 1.43†	4.12 ± 1.17
	Δ%	0	21 ± 29†	20 ± 29†	23 ± 32
Diameter	mm	3.10 ± 0.54	3.08 ± 0.54	3.06 ± 0.54†	3.22 ± 0.42
	Δ%	0	−1.8 ± 3.3	−2.5 ± 2.5†	−3.1 ± 2.1
CBF	ml min^{-1}	73 ± 31	67 ± 28	74 ± 38	83 ± 37
	Δ%	0	−10 ± 15	−2 ± 22	−9 ± 22
CVR	mmHg min ml^{-1}	1.59 ± 0.95	1.86 ± 1.07†	1.87 ± 1.17†	1.45 ± 0.50
	Δ%	0	28 ± 28†	29 ± 32†	37 ± 41
Global (ICA+VA)					
CBF	ml min^{-1}	299 ± 73	287 ± 72	294 ± 80	334 ± 55
	Δ%	0	−5 ± 12	−3 ± 13	−9 ± 7
CVR	mmHg min ml^{-1}	0.33 ± 0.11	0.37 ± 0.10†	0.39 ± 0.13†	0.32 ± 0.05
	Δ%	0	19 ± 18†	26 ± 24†	29 ± 9

Values are mean ± SD, $^{\dagger}P < 0.05$, comparisons with the baseline using one-way repeated-measures ANOVA with Bonferroni correction for *post hoc* tests. Note that statistical analyses were performed only at the dosages of 0.50 and 1.0 μg kg^{-1} min^{-1} because fewer subjects had high dosages. See Table 2 for other definitions.

Table 4. Regional and global CA measured with different metrics using linear regression slope

CA slope		Regional			
		Anterior		Posterior	Global
y (Δ%)	*x*	MCA	ICA	VA	ICA+VA
Doppler US					
CBFV	MAP (mmHg)	0.21 ± 0.39	0.23 ± 0.34	0.36 ± 0.56	
	MAP (Δ%)	0.19 ± 0.37	0.21 ± 0.33	0.32 ± 0.53	
CVRI	MAP (mmHg)	0.94 ± 0.51	0.91 ± 0.41	0.86 ± 0.75	
	MAP (Δ%)	0.85 ± 0.46	0.82 ± 0.36	0.78 ± 0.70	
Duplex US					
CBF	MAP (mmHg)		0.00 ± 0.45*	0.04 ± 0.65*	0.02 ± 0.42
	MAP (Δ%)		0.00 ± 0.42*	0.04 ± 0.60*	0.02 ± 0.38
CVR	MAP (mmHg)		1.21 ± 0.62*	1.25 ± 0.90*	1.18 ± 0.57
	MAP (Δ%)		1.08 ± 0.53*	1.13 ± 0.84*	1.06 ± 0.48

Values are mean ± SD ($n = 27$ for ICA and VA; $n = 24$ for MCA due to three subjects who did not have an adequate temporal window for TCD). *$P < 0.05$, comparisons of CA metrics between the measurements of CBFV and CBF (or between CVRI and CVR) for the same artery with paired *t*-tests. CA, cerebral autoregulation; Δ%, percentage change relative to baseline; MCA, middle cerebral artery; ICA, internal carotid artery; VA, vertebral artery; US, ultrasonography; MAP, mean arterial pressure; CBFV, cerebral blood flow velocity; CVRI, cerebrovascular resistance index (= MAP/CBFV); CBF, cerebral blood flow; CVR, cerebrovascular resistance (= MAP/CBF).

one-third of individuals who had changes in CBF in an opposite direction from that of changes in arterial pressure. These observations challenge the traditional concept of CA which suggests that CBF would remain relatively constant during moderate changes in arterial pressure in healthy individuals. Furthermore, we found that posterior CA as quantified by the ΔCVR%–ΔMAP% slopes was correlated positively with WMH, and that CA slopes were much steeper in those who had high PWMH (> 0.3 %ICV) than those with low or moderate PWMH

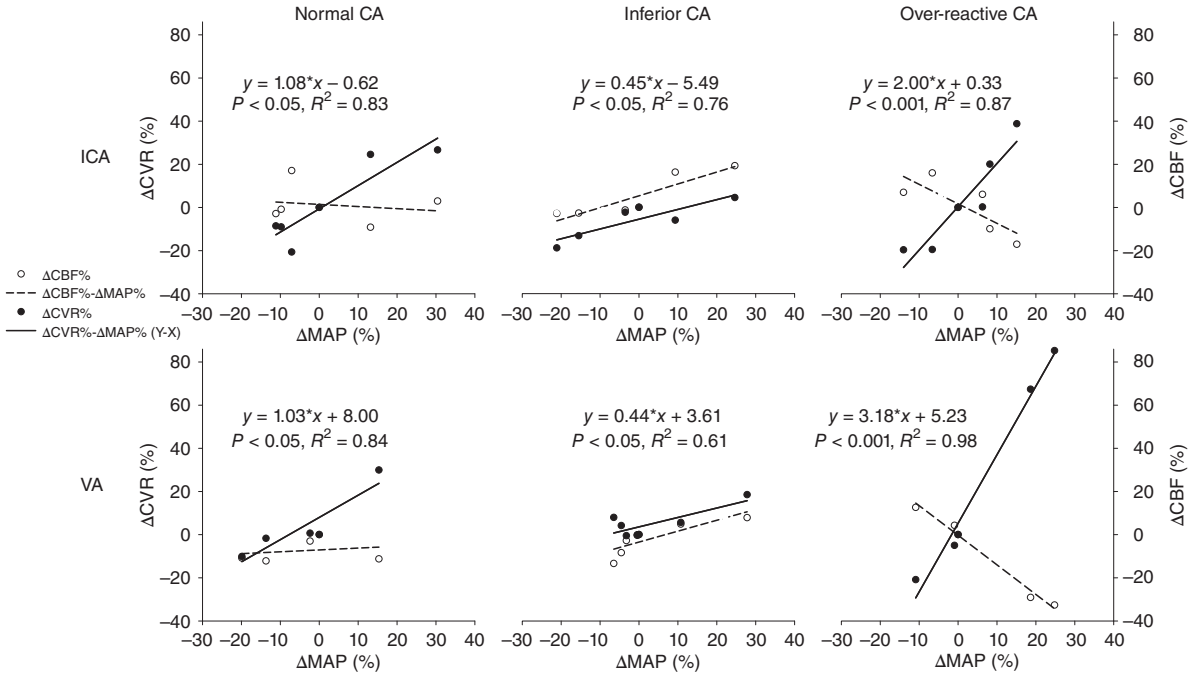

Figure 1. Three typical patterns of (normal, inferior, over-reactive) CA measured at ICA (upper row) and VA (bottom row)
CA, cerebral autoregulation; ICA, internal carotid artery; VA, vertebral artery; CBF, cerebral blood flow; MAP, mean arterial pressure; CVR, cerebrovascular resistance (= MAP/CBF). Open circles represent the percentage change of CBF from baseline (ΔCBF%), and solid circles represent CVR (ΔCVR%); the dashed lines show the trend of changes in ΔCBF%, and the continuous lines show changes in ΔCVR%. The CA slope between ΔCVR% and ΔMAP% is calculated as the regression coefficient from each of the estimated equations.

(≤ 0.3 %ICV), suggesting that the presence of cerebral SVD, manifested as WMH, is associated with posterior brain hypoperfusion during acute increase in arterial pressure. Collectively, these findings provide new insights into CA and its relationship with brain WMH in older adults. In the following, we discuss the methods used to assess CA and the potential mechanisms underlying these findings.

Methodological considerations

Previous studies of CA used either the direct or the indirect tracer methods for CBF measurement, which include single photon emission computed tomography, positron emission tomography, perfusion computed tomography or MRI (Van Beek *et al.* 2008; Gould *et al.* 2013). These methods overall had low temporal resolution, could be invasive and were difficult to implement in clinical studies (Wintermark *et al.* 2005). Recently, TCD has been used extensively to assess CA because of its high temporal resolution, relatively low cost and non-invasive properties (Aries *et al.* 2010). However, TCD measures only CBFV, which may underestimate CA as shown in the present and previous studies (Liu *et al.* 2013; Lewis *et al.* 2015). In the present study, volumetric CBF was measured at the ICA and VA using duplex ultrasonography. This technology has the advantage of combining both blood flow velocity and vessel diameter measurements to quantify changes in CBF in the major cerebral feeding arteries, and thus is arguably the currently most feasible and reliable method for assessing CA in human subjects (Liu *et al.* 2013). Of note, changes in CBF measured at the ICA and VA are likely to reflect mainly the downstream vascular bed CA properties as changes of the ICA and VA diameters in response to either decreases or increases in arterial pressure were relatively small (~ 1–3%, Tables 2 and 3) (Liu *et al.* 2013).

Under normal physiological conditions, CBFs measured at the ICA and VA represent the anterior and posterior cerebral circulation, respectively, despite the presence of the circle of Willis and other downstream collateral circulations (Hendrikse *et al.* 2004). However, the presence of intracranial stenosis and/or anatomical variations of the circle of Willis may have significant impact on regional CBF distribution, thus confounding the reliability of regional CA assessments with the use of ultrasonography. To reduce these potential confounding effects, individuals with moderate to severe carotid or vertebral arterial stenosis (> 50%) were excluded; moreover, the waveform profiles of CBFV observed at the MCA, ICA and VA all had normal values and the expected directions from normal individuals. Thus, individuals of the present study were less likely to have severe intracranial stenosis. Anatomical variations of the circle of Willis are common even in healthy individuals (> 50%) (Bergman *et al.* 2000). However, most of these variations are related to the ICA supply to the posterior circulation, while the VA supply to the anterior circulation is rare (Bergman *et al.* 2000;

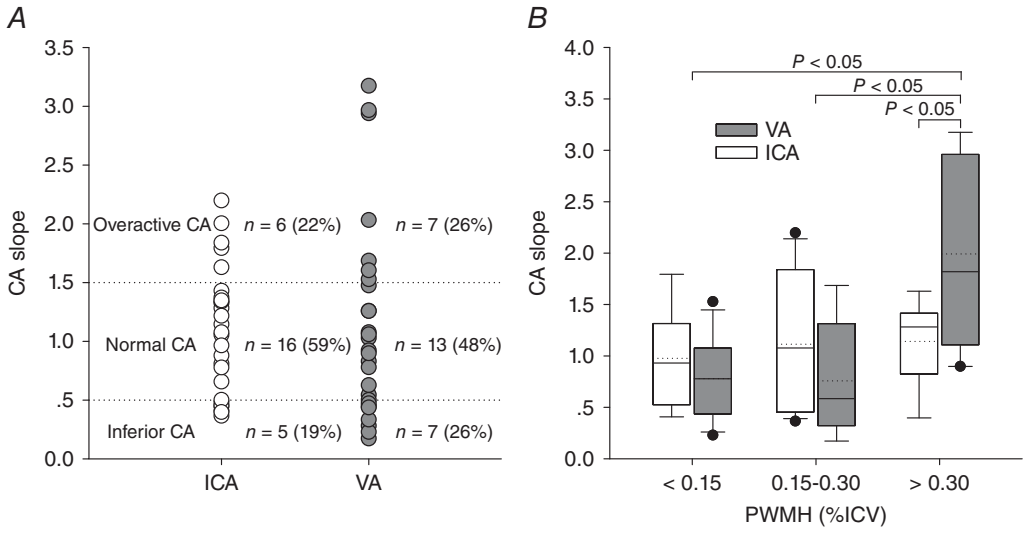

Figure 2. Individual variability of regional CA slopes and its association with PWMH
A, scatter plots of CA slopes at ICA and VA. The individual variability of CA slopes at both the ICA and the VA has a normal distribution by the Kolmogorov–Smirnov test with no differences between mean values. *B*, box plots of CA slopes in the ICA and VA between the tertiles of PWMH. The CA slope measured at the VA in the group with high PWMH (> 0.3 %ICV, $n = 8$) was much greater than that at the ICA and those at the VA or ICA in the groups with low (< 0.15 %ICV, $n = 8$) and moderate (0.15–0.30 %ICV, $n = 11$) PWMH. The horizontal dotted and continuous lines within the box represent the mean and median, respectively. CA, cerebral autoregulation; ICA, internal carotid artery; VA, vertebral artery; PWMH, periventricular white matter hyperintensity; %ICV, percentage of intracranial volume.

Table 5. Correlation matrix between systemic variables, CA metrics and WMH

	Systemic variables					CA slope (Δ%–ΔMAP%)								WMH (%ICV)		
Variables	Sex	VRFs	Anti-HTN	SBP	Aortic PWV	$CBFV_{MCA}$	$CVRI_{MCA}$	CBF_{ICA}	CVR_{ICA}	CBF_{VA}	CVR_{VA}	CBF_{ICA+VA}	CVR_{ICA+VA}	TWMH	PWMH	DWMH
Age	−0.01	−0.01	−0.23	0.15	**0.50**‡	0.04	−0.01	−0.16	0.17	**−0.40**†	**0.46**†	−0.24	0.26	**0.43**†	**0.45**†	0.05
Sex		0.23	0.20	**0.39**†	0.03	−0.17	0.23	−0.11	0.11	**0.31***	−0.23	0.00	0.03	**−0.40**†	**−0.49**‡	−0.11
VRFs			**0.78**$^{\#}$	**0.35***	0.10	−0.10	0.14	−0.10	0.15	0.01	0.06	−0.12	0.12	−0.01	−0.11	0.17
Anti-HTN				0.27	0.00	−0.11	0.17	−0.12	0.19	0.17	−0.12	−0.07	0.12	−0.02	−0.10	0.12
SBP					**0.45**†	0.12	−0.13	0.09	−0.18	−0.08	0.18	0.05	−0.10	**0.32***	0.27	**0.30***
Aortic PWV						−0.22	0.15	**−0.30***	0.20	**−0.37***	**0.45**†	**−0.38***	**0.29***	**0.56**‡	**0.51**‡	**0.41**†
$CBFV_{MCA}$							**−0.97**$^{\#}$	**0.80**$^{\#}$	**−0.75**$^{\#}$	0.11	−0.09	**0.71**$^{\#}$	**−0.65**‡	−0.10	−0.04	−0.20
$CVRI_{MCA}$								**−0.78**$^{\#}$	**0.80**$^{\#}$	−0.10	0.10	**−0.69**$^{\#}$	**0.70**$^{\#}$	0.03	−0.01	0.12
CBF_{ICA}									**−0.95**$^{\#}$	**0.40**†	**−0.37***	**0.94**$^{\#}$	**−0.88**$^{\#}$	**−0.35***	**−0.34***	−0.14
CVR_{ICA}										**−0.35***	**0.36***	**−0.89**$^{\#}$	**0.93**$^{\#}$	0.26	0.27	0.04
CBF_{VA}											**−0.95**$^{\#}$	**0.67**$^{\#}$	**−0.62**‡	**−0.66**$^{\#}$	**−0.69**$^{\#}$	−0.10
CVR_{VA}												**−0.64**$^{\#}$	**0.65**$^{\#}$	**0.72**$^{\#}$	**0.74**$^{\#}$	0.13
CBF_{ICA+VA}													**−0.94**$^{\#}$	**−0.52**‡	**−0.52**‡	−0.17
CVR_{ICA+VA}														**0.46**†	**0.47**†	0.10
TWMH															**0.98**$^{\#}$	**0.42**†
PWMH																0.22

Values are expressed as the Pearson's product moment correlation coefficient for continuous variables or Spearman's rank correlation coefficient for categorical variables (Sex, VRFs and Anti-HTN). Values with $P < 0.15$ are highlighted in bold, where $^{*}P < 0.15$, $^{†}P < 0.05$, $^{‡}P < 0.01$ and $^{\#}P < 0.001$. CA, cerebral autoregulation; Δ%, percentage change relative to baseline; MAP, mean arterial pressure; WMH, white matter hyperintensity; %ICV, percentage of intracranial volume; VRFs, vascular risk factors; Anti-HTN, anti-hypertensive medications; SBP, systolic blood pressure; Aortic PWV, carotid–femoral pulse wave velocity; CBFV, cerebral blood flow velocity; CVRI, cerebrovascular resistance index (= MAP/CBFV); CBF, cerebral blood flow; CVR, cerebrovascular resistance (= MAP/CBF); MCA, middle cerebral artery; ICA, internal carotid artery; VA, vertebral artery; PWMH, periventricular WMH; DWMH, deep WMH; TWMH, total WMH (= PWMH + DWMH). Sex is coded as 0 for female and 1 for male; the score of VRFs is coded as 0 for no risk factors, 1 for treated hypertension or hypercholesterolaemia and 2 for both factors; Anti-HTN is coded as 0 for no use and 1 for use.

Hoksbergen *et al.* 2000). Thus, changes in CBF at the VA would reflect mainly posterior circulation, which support the data interpretation of this study. Future studies using MRI or computed tomography angiography may provide additional information on the effect of anatomical variants of the intracranial vessels on regional CA measurements.

Traditionally, assessment of CA has focused on the description of the relationship between changes in MAP and CBF (Tan & Taylor, 2014; Tzeng & Ainslie, 2014). In the present study, CA was assessed using the linear regression slopes of Δ% in CBFV, CBF, CVRI or CVR *versus* either absolute or Δ% changes in MAP with a focus on the ΔCVR%–ΔMAP% relationship. One of the rationales behind use of these metrics to assess CA was to reveal if the observations of the study were influenced by the specific methods used to quantify CA. Theoretically, arterial pressure, blood flow and vascular resistance are intrinsically related to each other governed by Poiseuille's law under laminar flow conditions (analogous to Ohm's law). Thus, assessment of CA using different metrics reflects different facets of CA which should complement rather than conflict each other, as demonstrated in the present study. We focused on the ΔCVR%–ΔMAP% relationship to assess CA because CVR is determined mainly by the physical properties of vascular beds such as vessel diameter, which is modulated by CA (Liu *et al.* 2013).

One additional advantage of using the ΔCVR%–ΔMAP% relationship to quantify CA is that a CA slope of 1 would correspond to a perfect CA (i.e. ΔCVR% equals ΔMAP% for a constant CBF), while a value of 0 corresponds to the absence of CA (i.e. ΔCBF% equals ΔMAP% without any changes in CVR), and thus facilitated the classification and comparisons of the individual CA variability observed in this study.

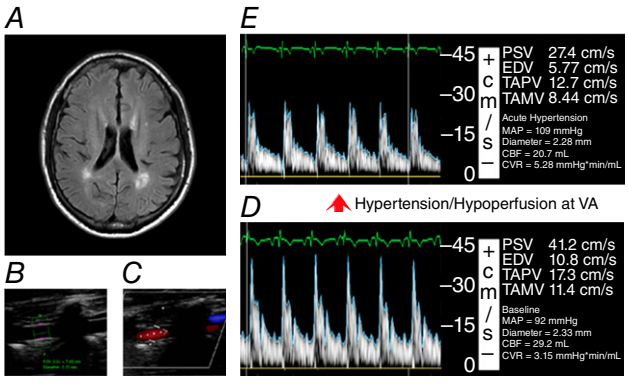

Figure 3. An increase in arterial pressure induced a paradoxical hypoperfusion, indicating over-reactivity of CA, measured at the VA in a 78-year-old male subject with prominent PWMH
A, representative FLAIR image showing salient PWMH (0.565 %ICV). *B*, the diameter of VA was measured in a longitudinal view on high-resolution B-mode video using automated software. *C*, the pulsed Doppler sampling volume was placed on the site of diameter measurement in colour mode. *D*, Doppler measurement of blood flow velocity at the VA when MAP was 92 mmHg at baseline. *E*, blood flow velocity at the VA was reduced when MAP elevated to 109 mmHg by intravenous infusion of phenylephrine with an estimated CA slope of 3.18. CA, cerebral autoregulation; VA, vertebral artery; PWMH, periventricular white matter hyperintensity; FLAIR, fluid-attenuated inversion recovery; %ICV, percentage of intracranial volume; PSV, peak systolic velocity; EDV, end-diastolic velocity; TAPV, time-averaged peak velocity; TAMV, time-averaged mean velocity; MAP, mean arterial pressure; CBF, volumetric cerebral blood flow; CVR, cerebrovascular resistance (= MAP/CBF).

Individual variability in CA

The description of 'cerebral autoregulatory plateau' has been a widely accepted dogma to indicate the presence of a normal CA (Lassen, 1959). However, this study showed that such an 'autoregulatory plateau' was absent in about 50% of healthy older adults who had either an 'inferior' or an 'over-reactive CA'. These observations extended previous studies by demonstrating the presence of large individual variability of CA during moderate changes in arterial pressure (Jones *et al.* 2002; Liu *et al.* 2013).

The presence of individual CA variability was often either ignored or under-reported (Jones *et al.* 2002). Description of CA was usually based on the pooled group data to show an autoregulatory plateau (i.e. CA slope ≈ 1, which is consistent with the observation of the present study). The large individual CA variability observed in this study argues against the contention that any variations from an autoregulatory plateau would suggest an impaired or abnormal CA capacity (Mutch *et al.* 1994).

We arbitrarily classified individual CA variability into the tertiles, i.e. an apparently normal, an inferior and an over-reactive CA. The underlying mechanisms for the observed CA individual variability are not known. Previous studies showed that CA is related to an array of complex regulatory mechanisms including endothelial, myogenic and metabolic regulation of cerebral arteries and/or arterioles in response to changes in arterial pressure (Tzeng & Ainslie, 2014). Furthermore, both intrinsic and extrinsic neural control mechanisms may play a role (Liu *et al.* 2013; Ainslie & Brassard, 2014). The observation of a positive correlation between aortic PWV and CA slopes measured at the VA in the present study suggests that increases in arterial stiffness and/or cerebrovascular tone also may contribute to CA individual variability. It is possible that an exaggerated CA vasodilatation or vasoconstriction associated with increases in arterial stiffness may lead to changes in CBF in an opposite direction from that of changes in arterial pressure. However, relative contributions of these regulatory mechanisms to CA individual variability are unknown. Previous studies in animals observed a paradoxical increase in brain perfusion during hypotension that was attributed to the presence

Table 6. Responses of CBFV, CBF, $ETCO_2$, ICA and VA diameters to changes in arterial pressure among the tertiles of PWMH

Linear regression slope		PWMH		
y (Δ%)	*x* (Δ%)	Low (< 0.15 %ICV), $n = 8$	Moderate (0.15–0.30 %ICV), $n = 11$	High (> 0.30 %ICV), $n = 8$
$CBFV_{MCA}$	MAP	0.18 ± 0.23	0.19 ± 0.49	0.21 ± 0.40
CBF_{ICA}	MAP	0.09 ± 0.39	0.01 ± 0.48	−0.11 ± 0.39
CBF_{VA}	MAP	0.32 ± 0.48	0.28 ± 0.28	−0.58 ± 0.63*
CBF_{ICA+VA}	MAP	0.14 ± 0.39	0.09 ± 0.35	−0.19 ± 0.37
$ETCO_2$	MAP	0.17 ± 0.32	0.05 ± 0.19	0.29 ± 0.23
D_{ICA}	MAP	−0.12 ± 0.11	−0.11 ± 0.11	−0.12 ± 0.09
D_{VA}	MAP	−0.12 ± 0.12	−0.08 ± 0.10	−0.15 ± 0.19

Values are mean ± SD. Note that three subjects did not have an adequate temporal window for TCD, and thus $n = 8$, 9 and 7 for the low, moderate and high PWMH, respectively. *$P < 0.05$, comparisons of high *vs.* low or moderate PWMH. CBFV, cerebral blood flow velocity; CBF, cerebral blood flow; $ETCO_2$, partial pressure of end-tidal carbon dioxide; ICA, internal carotid artery; VA, vertebral artery; PWMH, periventricular white matter hyperintensity; Δ%, percentage change relative to the baseline; %ICV, percentage of intracranial volume; MCA, middle cerebral artery; MAP, mean arterial pressure; D_{ICA}, ICA diameter; D_{VA}, VA diameter.

of hyper-reactivity of cerebral vascular responses (Jones *et al.* 2002). Furthermore, intensive anti-hypertensive treatment increased rather than reduced CBF, suggesting an over-reactive CA although the underlying mechanisms may be different from those observed in the present study (Tryambake *et al.* 2013).

Individual differences in cerebral vasomotor reactivity to changes in arterial CO_2 also may contribute to the observed CA individual variability. If this is the case, a decrease in $ETCO_2$ during reduction in arterial pressure would counteract CA vasodilatation, and vice versa during increases in arterial pressure (Liu *et al.* 2013). These events then might explain the presence of a less effective CA in some individuals, but not the over-reactivity of CA. Future studies with a clamped $ETCO_2$ during changes in arterial pressure may be valuable to address this question.

We cannot exclude the possibility that individual cerebrovascular responses to the vasoactive drugs used may have contributed to the observed CA variability. For example, SNP may cause direct cerebral vasodilatation, and interact with CA, leading to CA variability. In addition, random measurement errors may contribute to the observed variability. Regardless of the underlying mechanisms, the potential clinical significance of CA individual variability needs to be better understood regarding its role in the protection of brain perfusion (Panerai, 2008).

Regional CA

Few studies have compared anterior and posterior CA in older subjects (Haubrich *et al.* 2004; Sorond *et al.* 2005; Reinhard *et al.* 2008; Nakagawa *et al.* 2009). Measurement of CBFV using TCD at the MCA and posterior cerebral artery (PCA) suggested that posterior CA was less effective than anterior CA (Haubrich *et al.* 2004; Sorond *et al.* 2005). However, these findings are inconsistent (Reinhard *et al.* 2008; Nakagawa *et al.* 2009).

In the present study, we found no differences between the anterior (MCA, ICA) and posterior CA (VA) regardless of CA metrics used. However, CA individual variability measured at the VA was larger than that of the ICA. In addition, there appeared to be a weak correlation between the anterior and posterior CA ($r = 0.36$, $P = 0.07$) assessed with the ΔCVR%–ΔMAP% slopes at the ICA and VA (Table 5). These observations suggest that regional differences in CA, if they do exist, are likely to be manifested at the individual rather than the group level (Baumbach & Heistad, 1985).

CA and WMH

WMH is commonly seen in older adults and is likely to be heterogeneous in origin; current evidence indicates that it reflects mainly the presence of cerebral SVD (Wen & Sachdev, 2004; Wardlaw *et al.* 2013). Previous studies suggested that impaired CA may contribute to the development of WMH (Pantoni & Garcia, 1997; Joutel *et al.* 2010). However, only a few studies have been performed in human subjects (Matsushita *et al.* 1994; Birns *et al.* 2009; Purkayastha *et al.* 2013). One study in hypertensive patients showed an association between impaired static CA and PWMH (Matsushita *et al.* 1994); while others did not find correlations between dynamic CA and WMH (Birns *et al.* 2009; Purkayastha *et al.* 2013). In this study, we did not find associations between steady-state assessments of CA at the ICA and WMH. However, CA measured at the VA showed a positive correlation with PWMH, and high PWMH (> 0.3 %ICV) was associated with over-reactivity of CA.

Whether the association between PWMH and posterior CA represents an epiphenomenon or suggests a potential pathophysiological mechanism cannot be determined in

this study. This association was observed even after the adjustment for age, sex, SBP and aortic PWV. In addition, this association was unlikely to be due to the differences in the regulatory mechanisms of the large cerebral arteries as the regression slopes of changes in $ETCO_2$, and ICA and VA diameters in response to changes in arterial pressure were similar among the three PWMH groups.

Why then was the PWMH but not the DWMH correlated with the posterior CA? Several possibilities exist. First, PWMH is likely to be related more closely to a vascular mechanism such as hypoperfusion or ischaemic insults than DWMH (ten Dam *et al.* 2007). Second, although both ICA (via MCA and anterior cerebral artery) and VA (via PCA) supply blood flow to the periventricular white matter regions, SVD as revealed by PWMH may be more sensitive to alterations of CBF in the posterior than anterior circulation. For example, a paradoxical reduction in CBF in the posterior cerebral circulation during acute increases in arterial pressure may contribute to the development of WMH. Conversely, the presence of SVD in the periventricular regions may affect CA to a larger extent in the posterior than anterior circulation. Finally, differences in regional blood–brain barrier permeability may result in the posterior circulation being more sensitive to the vasoactive drugs used in this study (Tomimoto *et al.* 1996). Of note, CA slopes measured at either the VA or the ICA did not have an expected negative correlation with WMH, which would suggest that a less effective or impaired CA is related to WMH (Pantoni & Garcia, 1997; Joutel *et al.* 2010). The presence of individual capability of brain tissue oxygen extraction during hypoperfusion and/or other compensatory mechanisms may explain these observations.

The potential clinical implications of the observed over-reactivity of posterior CA associated with the severity of PWMH need to be discussed. For example, the incidence of posterior circulation ischaemia increases significantly with advanced age (Caplan *et al.* 2004), causing not only symptoms such as dizziness and vision problems, but also falls that affect about 30% of people over age 65 years (Sloane *et al.* 1989). Thus, it is possible that the presence of posterior CA over-reactivity and hypoperfusion during acute increases in blood pressure in those with severe WMH may be one of the underlying mechanisms of posterior circulation ischaemia and falls in older adults.

Strengths and limitations

The strength of this study is the quantitative assessment of CA during well-controlled stepwise changes in arterial pressure as well as the use of non-invasive duplex ultrasonography, which allowed us to perform sequential and repeated measurements of CBF. Another strength is the rigorous screening of the study participants, which reduced potential confounding effects of cardiovascular, neurological and other chronic conditions on CA and WMH (Pantoni & Garcia, 1997; Aries *et al.* 2010; Wardlaw *et al.* 2013). Finally, a comprehensive measurement of vascular risk variables allowed us to explore the relationship between regional CA and WMH after accounting for covariates such as age, sex, aortic stiffness, baseline blood pressure and use of anti-hypertensive medication (Sorond *et al.* 2005; King *et al.* 2013; Purkayastha *et al.* 2013).

However, as discussed above, potential direct effects of vasoactive drugs on the cerebral vasculature could not be assessed and the lack of non-pharmacological interventions to induce changes in arterial pressure under steady-state conditions is a limitation of study of CA (Tzeng & Ainslie, 2014). Both SNP and phenylephrine are used commonly under clinical conditions for acute control of arterial pressure. Thus, the findings of this study have direct clinical implications even though a 'pure CA' may not be measured under current conditions. In addition, although regional CA was assessed at the MCA, ICA and VA using ultrasonography, we cannot assess associations between regional CA and WMH with higher spatial resolutions. Using MRI arterial spin labelling to measure local brain perfusion may be considered in future studies (Bokkers *et al.* 2010). Finally, the limitations of the small sample size and cross-sectional nature of the study should be acknowledged and the findings should be considered preliminary.

References

Ainslie P & Brassard P (2014). Why is the neural control of cerebral autoregulation so controversial? *F1000Prime Rep* **6**, 14.

Aries MJ, Elting JW, De Keyser J, Kremer BP & Vroomen PC (2010). Cerebral autoregulation in stroke: a review of transcranial Doppler studies. *Stroke* **41**, 2697–2704.

Bartko JJ (1994). Measures of agreement: a single procedure. *Stat Med* **13**, 737–745.

Baumbach GL & Heistad DD (1985). Regional, segmental, and temporal heterogeneity of cerebral vascular autoregulation. *Ann Biomed Eng* **13**, 303–310.

Bergman RA, Afifi AK & Miyauchi R (2000). *Illustrated Encyclopedia of Human Anatomic Variation.* University of Iowa, Iowa City, IA.

Birns J, Jarosz J, Markus HS & Kalra L (2009). Cerebrovascular reactivity and dynamic autoregulation in ischaemic subcortical white matter disease. *J Neurol Neurosurg Pyschiatry* **80**, 1093–1098.

Bokkers RP, van Osch MJ, van der Worp HB, de Borst GJ, Mali WP & Hendrikse J (2010). Symptomatic carotid artery stenosis: impairment of cerebral autoregulation measured at the brain tissue level with arterial spin-labelling MR imaging. *Radiology* **256**, 201–208.

Caplan LR, Wityk RJ, Glass TA, Tapia J, Pazdera L, Chang HM, Teal P, Dashe JF, Chaves CJ & Breen JC (2004). New England Medical Centre posterior circulation registry. *Ann Neurol* **56**, 389–398.

Chobanian AV, Bakris GL, Black HR, Cushman WC, Green LA, Izzo Jr JL, Jones DW, Materson BJ, Oparil S & Wright Jr JT (2003). The seventh report of the Joint National Committee on prevention, detection, evaluation, and treatment of high blood pressure: the JNC 7 report. *JAMA* **289**, 2560–2571.

DeCarli C, Fletcher E, Ramey V, Harvey D & Jagust WJ (2005). Anatomical mapping of white matter hyperintensities (WMH) exploring the relationships between periventricular WMH, deep WMH, and total WMH burden. *Stroke* **36**, 50–55.

Desikan RS, Segonne F, Fischl B, Quinn BT, Dickerson BC, Blacker D, Buckner RL, Dale AM, Maguire RP, Hyman BT, Albert MS & Killiany RJ (2006). An automated labelling system for subdividing the human cerebral cortex on MRI scans into gyral based regions of interest. *Neuroimage* **31**, 968–980.

Girouard H & Iadecola C (2006). Neurovascular coupling in the normal brain and in hypertension, stroke, and Alzheimer disease. *J Appl Physiol* **100**, 328–335.

Gould B, McCourt R, Asdaghi N, Dowlatshahi D, Jeerakathil T, Kate M, Coutts SB, Hill MD, Demchuk AM & Shuaib A (2013). Autoregulation of cerebral blood flow is preserved in primary intracerebral hemorrhage. *Stroke* **44**, 1726–1728.

Haubrich C, Wendt A, Diehl R & Klötzsch C (2004). Dynamic autoregulation testing in the posterior cerebral artery. *Stroke* **35**, 848–852.

Hendrikse J, van der Grond J, Lu H, van Zijl PC & Golay X (2004). Flow territory mapping of the cerebral arteries with regional perfusion MRI. *Stroke* **35**, 882–887.

Hoksbergen A, Legemate D, Ubbink DT & Jacobs M (2000). Collateral variations in circle of Willis in atherosclerotic population assessed by means of transcranial colour-coded duplex ultrasonography. *Stroke* **31**, 1656–1660.

Hoth KF, Tate DF, Poppas A, Forman DE, Gunstad J, Moser DJ, Paul RH, Jefferson AL, Haley AP & Cohen RA (2007). Endothelial function and white matter hyperintensities in older adults with cardiovascular disease. *Stroke* **38**, 308–312.

Jones SC, Radinsky CR, Furlan AJ, Chyatte D, Qu Y, Easley KA & Perez-Trepichio AD (2002). Variability in the magnitude of the cerebral blood flow response and the shape of the cerebral blood flow: pressure autoregulation curve during hypotension in normal rats. *Anesthesiology* **97**, 488–496.

Joutel A, Monet-Leprêtre M, Gosele C, Baron-Menguy C, Hammes A, Schmidt S, Lemaire-Carrette B, Domenga V, Schedl A & Lacombe P (2010). Cerebrovascular dysfunction and microcirculation rarefaction precede white matter lesions in a mouse genetic model of cerebral ischemic small vessel disease. *J Clin Invest* **120**, 433–445.

King KS, Chen KX, Hulsey KM, McColl RW, Weiner MF, Nakonezny PA & Peshock RM (2013). White matter hyperintensities: use of aortic arch pulse wave velocity to predict volume independent of other cardiovascular risk factors. *Radiology* **267**, 709–717.

Lam JM, Hsiang JN & Poon WS (1997). Monitoring of autoregulation using laser Doppler flowmetry in patients with head injury. *J Neurosurg* **86**, 438–445.

Lassen NA (1959). Cerebral blood flow and oxygen consumption in man. *Physiol Rev* **39**, 183–238.

Lewis NC, Smith KJ, Bain AR, Wildfong KW, Numan T & Ainslie PN (2015). Impact of transient hypotension on regional cerebral blood flow in humans. *Clin Sci* **129**, 169–178.

Liu J, Zhu Y-S, Hill C, Armstrong K, Tarumi T, Hodics T, Hynan LS & Zhang R (2013). Cerebral autoregulation of blood velocity and volumetric flow during steady-state changes in arterial pressure. *Hypertension* **62**, 973–979.

Liu J, Zhu Y-S, Khan MA, Brunk E, Martin-Cook K, Weiner MF, Cullum CM, Lu H, Levine BD & Diaz-Arrastia R (2014). Global brain hypoperfusion and oxygenation in amnestic mild cognitive impairment. *Alzheimers Dement* **10**, 162–170.

Lucas SJ, Tzeng YC, Galvin SD, Thomas KN, Ogoh S & Ainslie PN (2010). Influence of changes in blood pressure on cerebral perfusion and oxygenation. *Hypertension* **55**, 698–705.

Matsushita K, Kuriyama Y, Nagatsuka K, Nakamura M, Sawada T & Omae T (1994). Periventricular white matter lucency and cerebral blood flow autoregulation in hypertensive patients. *Hypertension* **23**, 565–568.

Mutch W, Sutton I, Teskey J, Cheang M & Thomson I (1994). Cerebral pressure–flow relationship during cardiopulmonary bypass in the dog at normothermia and moderate hypothermia. *J Cerebr Blood Flow Metab* **14**, 510–518.

Nakagawa K, Serrador JM, LaRose SL, Moslehi F, Lipsitz LA & Sorond FA (2009). Autoregulation in the posterior circulation is altered by the metabolic state of the visual cortex. *Stroke* **40**, 2062–2067.

Ogoh S, Brothers RM, Barnes Q, Eubank WL, Hawkins MN, Purkayastha S & Raven PB (2005). The effect of changes in cardiac output on middle cerebral artery mean blood velocity at rest and during exercise. *J Physiol* **569**, 697–704.

Panerai RB (2008). Cerebral autoregulation: from models to clinical applications. *Cardiovasc Eng* **8**, 42–59.

Pantoni L & Garcia JH (1997). Pathogenesis of leukoaraiosis a review. *Stroke* **28**, 652–659.

Paulson O, Strandgaard S & Edvinsson L (1990). Cerebral autoregulation. *Cerebr Brain Metab Rev* **2**, 161–192.

Purkayastha S, Fadar O, Mehregan A, Salat DH, Moscufo N, Meier DS, Guttmann CR, Fisher ND, Lipsitz LA & Sorond FA (2013). Impaired cerebrovascular hemodynamics are associated with cerebral white matter damage. *J Cerebr Blood Flow Metab* **34**, 228–234.

Reinhard M, Waldkircher Z, Timmer J, Weiller C & Hetzel A (2008). Cerebellar autoregulation dynamics in humans. *J Cerebr Blood Flow Metab* **28**, 1605–1612.

Rosano C, Watson N, Chang Y, Newman AB, Aizenstein HJ, Du Y, Venkatraman V, Harris TB, Barinas-Mitchell E & Sutton-Tyrrell K (2013). Aortic pulse wave velocity predicts focal white matter hyperintensities in a biracial cohort of older adults. *Hypertension* **61**, 160–165.

Sloane P, Blazer D & George LK (1989). Dizziness in a community elderly population. *J Am Geriatrics Soc* **37**, 101–108.

Sorond FA, Khavari R, Serrador JM & Lipsitz LA (2005). Regional cerebral autoregulation during orthostatic stress: age-related differences. *J Gerontol A Biol Sci Med Sci* **60**, 1484–1487.

Tan CO & Taylor JA (2014). Integrative physiological and computational approaches to understand autonomic control of cerebral autoregulation. *Exp Physiol* **99**, 3–15.

ten Dam VH, van den Heuvel DM, de Craen AJ, Bollen EL, Murray HM, Westendorp RG, Blauw GJ & van Buchem MA (2007). Decline in total cerebral blood flow is linked with increase in periventricular but not deep white matter hyperintensities. *Radiology* **243**, 198–203.

Thompson CS & Hakim AM (2009). Living beyond our physiological means small vessel disease of the brain is an expression of a systemic failure in arteriolar function: a unifying hypothesis. *Stroke* **40**, e322-e330.

Tomimoto H, Akiguchi I, Suenaga T, Nishimura M, Wakita H, Nakamura S & Kimura J (1996). Alterations of the blood–brain barrier and glial cells in white-matter lesions in cerebrovascular and Alzheimer's disease patients. *Stroke* **27**, 2069–2074.

Tryambake D, He J, Firbank M, O'Brien J, Blamire A & Ford G (2013). Intensive blood pressure lowering increases cerebral blood flow in older subjects with hypertension. *Hypertension* **61**, 1309.

Tseng B, Gundapuneedi T, Khan M, Diaz-Arrastia R, Levine B, Lu H, Huang H & Zhang R (2013). White matter integrity in physically fit older adults. *Neuroimage* **82**, 510–516.

Tzeng Y-C & Ainslie PN (2014). Blood pressure regulation IX: cerebral autoregulation under blood pressure challenges. *Eur J Appl Physiol* **114**, 545–559.

Van Beek AH, Claassen JA, Rikkert MGO & Jansen RW (2008). Cerebral autoregulation: an overview of current concepts and methodology with special focus on the elderly. *J Cerebr Blood Flow Metab* **28**, 1071–1085.

Wardlaw JM, Smith EE, Biessels GJ, Cordonnier C, Fazekas F, Frayne R, Lindley RI, O'Brien JT, Barkhof F & Benavente OR (2013). Neuroimaging standards for research into small vessel disease and its contribution to ageing and neurodegeneration. *Lancet Neurol* **12**, 822–838.

Wen W & Sachdev P (2004). The topography of white matter hyperintensities on brain MRI in healthy 60- to 64-year-old individuals. *Neuroimage* **22**, 144–154.

Wilkinson IB, Fuchs SA, Jansen IM, Spratt JC, Murray GD, Cockcroft JR & Webb DJ (1998). Reproducibility of pulse wave velocity and augmentation index measured by pulse wave analysis. *J Hypertens* **16**, 2079–2084.

Wintermark M, Sesay M, Barbier E, Borbély K, Dillon WP, Eastwood JD, Glenn TC, Grandin CB, Pedraza S & Soustiel J-F (2005). Comparative overview of brain perfusion imaging techniques. *Stroke* **36**, e83–e99.

Additional information

Conflict of interest

The authors report no disclosures relevant to the manuscript.

Author contributions

J.L.: data acquisition, statistical analysis, data interpretation and drafting of the manuscript. B.Y.T., M.A.K. and T.T.: data acquisition, analysis and interpretation. C.H. and N.M.: subject screening, cognitive data collection and study coordination. T.M.H., L.S.H. and R.Z.: study concept and experimental design, interpretation of data and study supervision. All authors edited and revised the manuscript and approved the final submission.

Funding

This study was supported in part by NIH grants R01AG033106 and R01HL102457.

Acknowledgements

We thank all our study participants for their willingness, time and effort devoted to this study and all members of the study team for their excellent support.